Examining the Link Between Oil Prices and Exchange Rates: A Time-Invariant VAR Model Approach

Stephane Ellis, 22218816, COMP0047

ABSTRACT

This paper identifies the U.S. as the major trading hub in the world using a barrels loaded dataset and the K-means algorithm. It investigates the causal relationship between oil prices and USD exchange rates using linear and nonlinear Granger-causality tests. Linear causality tests suggest that oil prices Granger-cause exchange rates, while the nonlinear model does not capture any causality. The study then utilises a vector autoregressive (VAR) model and Cholesky decomposition to identify causal relationships and impulse response functions, revealing the short-term impacts of shocks on variables. The paper concludes that while oil prices influence exchange rates, the relationship is not time-invariant.

Contents

1 Introduction **3**

2 Loaded Barrels Dataset **4**

2.1 Methodology & Data 4

2.2 Results and Discussion 5

3 Interactions between oil price and exchange rate **6**

3.1 Overview of Oil Price and Exchange Rate Dynamics 6

3.2 Data and Methodology 6

3.2.1 Analysis of Stochastic Properties 7

3.2.2 Granger Causality Analysis 8

3.2.3 Time-invariant VAR Model 11

3.3 Results 14

4 Conclusion **16**

1 Introduction

The objective of this project is to identify the complex dynamics of the global oil market by analysing multiple datasets, each serving a specific purpose. The first dataset, loaded barrels, is examined to identify major global trade hubs over the period 2012–2017. The results indicate that the United States emerges as the most important global trading hub in the oil market, exhibiting the highest trading volume. Despite the U.S. share of global economic output declining from 32% in 1980 to 24% in 2020, the dollar's dominance in global trade remains strong [13]. Between 1999 and 2019, the Federal Reserve estimated that the dollar accounted for 96% of trade invoicing in the Americas, 74% in the Asia-Pacific region, and 79% globally, including oil transactions [3]. As a result, exchange rates play a critical role in both the global economy and the oil market.

This study explores the dynamic interactions between the spot oil price and the Real Trade Weighted U.S. Dollar Index (RTWUSD), a weighted average of the U.S. dollar relative to a basket of major currencies [1]. The weights are based on the relative trade balance of each country's currency against the others in the index. For instance, an increase in a country's currency exchange rate signals that its exports are becoming more expensive, while its imports become cheaper, indicating a loss of trade competitiveness [14]. The relationship between oil prices and exchange rates, analysed over the period from January 1986 to January 2019, reveals a fluctuating correlation over time. The variables show an inverse relationship during certain periods, while moving in tandem at other times. A correlation value of -0.45 is calculated over the entire period, prompting further investigation using rolling correlations to assess how the relationship strengthens or weakens across different intervals, with macroeconomic events considered as possible explanatory factors.

A key finding from the rolling correlation analysis is that the oil price and the RTWUSD exhibit stronger negative correlation between 2005 and 2019, influenced by the global financial crisis and increasing oil supply. To further analyse the dynamics, a time-invariant vector autoregressive (VAR) model is employed, which reveals that a sudden appreciation of the U.S. dollar leads to a significant decline in oil prices. The VAR model's impulse response functions show that shocks to the exchange rate generate a temporary, but significant, negative impact on oil prices. Conversely, oil price shocks lead to a brief depreciation of the dollar, but the effect dissipates within a few months.

These results provide valuable insights for investors, particularly regarding how exchange rate shocks may influence oil prices, thus offering guidance for optimising the risk-return profile of their portfolios.

2 Loaded Barrels Dataset

2.1 Methodology & Data

The first dataset contains the number of barrels loaded onto ships *per week*, departing from an origin port to a destination port. Additional features include the number of ships making the same journey in that week, the ship's port of origin, the year, the name of the previous port reached, and geographic details of each port, such as country and continent names. The dataset comprises 251,195 rows across 12 columns, with 128,423 missing values in the column for the number of barrels shipped. Various methods for addressing these missing values could be employed, including backfilling, which would require seasonality checks to ensure reasonable approximations. While median filling is also a common technique, it risks introducing lookahead bias if future values are used. Given the use of all years in the dataset for this analysis, and the approximately uniform distribution of missing values across the years, all missing values were removed. Certain ports of origin had entirely missing values for barrels, indicating a systematic data issue. The final dataset used for analysis contained 122,714 rows.

To identify the major trading hubs, the K-means clustering algorithm was employed, focusing on two key features: total trade volume and the number of trading partners for each country. The input data were first standardised using the `StandardScaler` [19] to ensure the features were on a comparable scale. The optimal number of clusters was determined using the elbow method, where inertia (the within-cluster sum of squares) was evaluated for various values of k. Figure 1 (left) shows the elbow plot, with the "elbow point" indicating the optimal k value, where the rate of decrease in inertia noticeably slows down.

After determining the optimal $k = 3$, the K-means algorithm was applied to cluster the standardised data. Each country was assigned to one of the clusters based on its trade volume and trading partners. Figure 1 (right) presents a bubble plot, where each bubble represents a country, sized according to its total trade volume and coloured by its cluster membership. This visualisation highlights the distribution of countries across clusters and the major trading hubs.

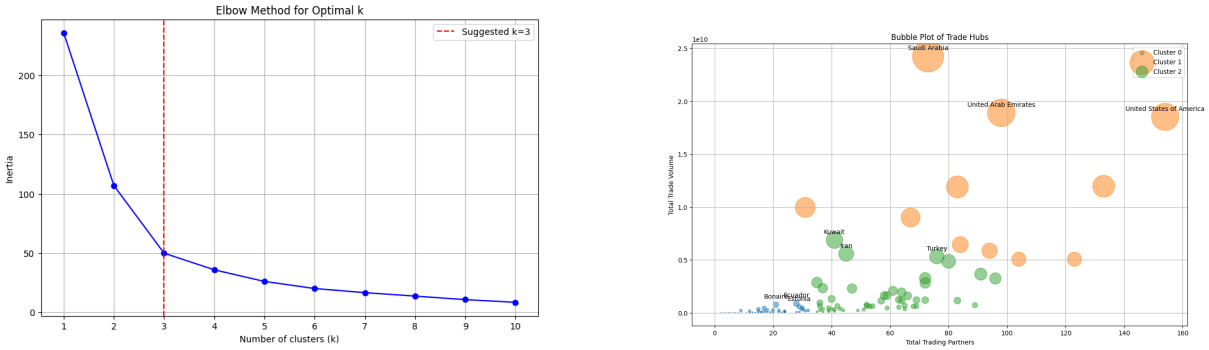

Figure 1: Panel (left) shows the inertia values for different numbers of clusters (k) using the elbow method, with the red dashed line indicating the optimal k value. Panel (right) visualises the major trading hubs using a bubble plot, where each bubble is proportional to total trade volume and coloured by cluster membership.

2.2 Results and Discussion

Table 1: Top 5 Country Trading Data

Country	Total Trade Volume	Total Trading Partners
Saudi Arabia	2.42×10^{10}	73.0
United Arab Emirates	1.89×10^{10}	98.0
United States of America	1.85×10^{10}	154.0
Singapore	1.20×10^{10}	133.0
Russia	1.19×10^{10}	83.0

Despite ranking third in total trade volume globally, the U.S. has the highest number of trading partners. This is clearly illustrated in the bubble plot, where the U.S. is positioned near the top right corner, indicating its prominence among both oil-importing and oil-exporting nations. This positioning reinforces the relevance of analysing the interactions between the U.S. Real Trade Weighted Exchange Rate (RTWUSD) and oil prices.

3 Interactions between oil price and exchange rate

3.1 Overview of Oil Price and Exchange Rate Dynamics

Market participants outside the U.S. purchase oil using USD. When the USD appreciates, they need to exchange more of their domestic currency for the same amount of oil, reducing USD reserves in oil-importing countries and leading to current account imbalances and portfolio adjustments [4]. This increases demand for USD, while the supply of foreign currencies rises. As a result, the USD strengthens, and the exchange rate declines. For example, an exchange rate of 1 means 1 unit of USD equals 1 unit of foreign currency, whereas a lower rate, such as 0.5, indicates that 0.5 USD is required for 1 unit of foreign currency, reflecting an increase in USD purchasing power.

A depreciation of the USD can lead to higher global oil prices, resulting in a negative correlation for two reasons: (i) an increase in oil demand from oil-importing countries, accompanied by a reduction in supply from oil-exporting regions; and (ii) lower returns on USD-denominated financial assets, which make commodities like oil more attractive due to portfolio rebalancing dynamics.

3.2 Data and Methodology

First, the historical USD exchange rates, measured against a broad basket of currencies from January 1986 until February 2019, were obtained. The same process was applied to WTI crude oil prices, and the values were indexed to January 2000 as outlined by jkclem [16]. The natural logarithm of both variables was taken, as the difference between two consecutive values would yield growth rates.

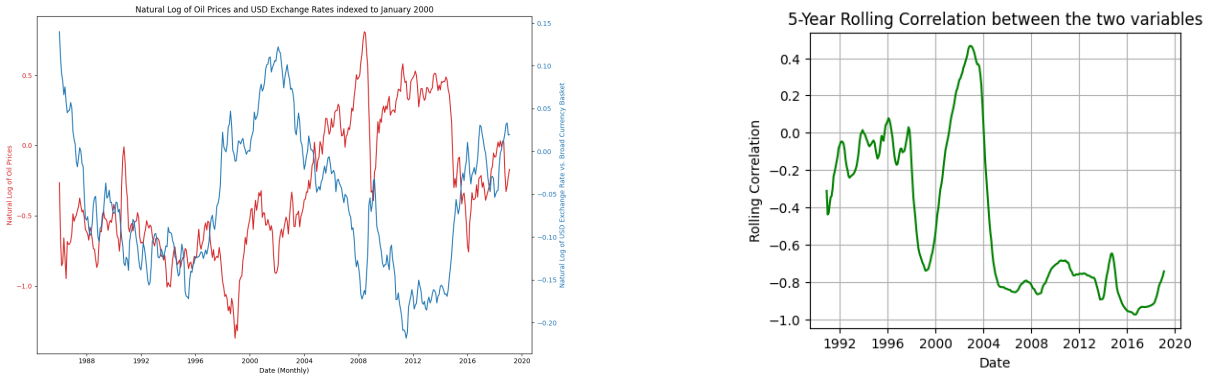

Figure 2: Panel (left) shows the log of WTI Crude Oil prices and the log of the Real Trade Weighted U.S. Dollar Index over time. Panel (right) depicts the 5-year rolling correlation between the log of WTI Crude Oil prices and the log of the Real Trade Weighted U.S. Dollar Index over time.

The variables plotted in Figure 2(a) appear to be inversely related over time. A lagging correlation analysis, shown in Figure 2(b), was conducted to examine whether this inverse relationship persists. The plot indicates that the relationship between the two variables is not consistent over time. Prior to the year 2000, the variables appear weakly uncorrelated. However, between 2000 and 2004, the correlation strengthens, reaching values over 0.4. From 2005 until 2019, the correlation remains strong, ranging from -0.8 to -1.0.

Positive correlations dominate the period from 2000 to 2004, coinciding with strong growth in oil prices, which was driven by the economic boom in Asian markets. The pronounced weakness of the USD during the period between 2000 and 2008 also contributed to this trend [12]. The negative correlations observed from 2005 onwards are largely attributed to the global financial crisis of 2008 and a significant increase in global oil supply.

3.2.1 Analysis of Stochastic Properties

The stochastic properties of the time series were first examined using the Augmented-Dickey Fuller (ADF) test to check for stationarity. However, since the ADF test does not account for the possibility of structural breaks in the time series, an additional Zivot-Andrews test was performed, which allows for a single structural break in the series Eric [9]. Both tests suggest that the data is *I(1)*, indicating that the series become stationary after being differentiated once. After differentiation, the p-values fall below the 5% threshold, allowing rejection of the null hypothesis that the series contain a unit root with a single structural break.

Next, a structural break test was applied to the individual time series. If structural breaks were detected, a cointegration test allowing for an unknown number of structural breaks, as described by Maki [18], would be required. The detection of

structural breaks was carried out using the `ruptures` package [23]. The goal of the change point detection was to identify the points at which the mean of the time series changed. The Pelt algorithm, or "Pruned Exact Linear Time," addresses the challenge of detecting change points when the number of such points is uncertain. It achieves this by minimising a penalised sum of costs, with the penalty being a linear function of the number of change points. A penalty value of 5 and subsamples occurring every 10 periods were used. The test did not detect any structural breaks in either time series.

Following this, the Engle and Granger two-step procedure was applied as a cointegration test. This involves first estimating a cross-sectional regression and then testing the residuals from the regression using an ADF test with modified critical values. The cross-sectional regression is given by

$$Y_t = X_t\beta + D_t\gamma + \eta_t, \tag{3.1}$$

where Y_t and X_t represent the two variables being tested for cointegration, and D_t represents a set of deterministic regressors, such as a constant, a time trend, or a quadratic time trend.

The results of the cointegration test yielded a p-value of 0.689, which is high, indicating that the null hypothesis of no cointegration cannot be rejected. Therefore, the variables can be used in the analysis by taking the first differences of each series and incorporating them into the VAR model. Conducting this cointegration test is crucial because performing a VAR test without accounting for cointegration would be suboptimal if the series were, in fact, cointegrated. Cointegrated series move together in the long run, and a VAR model in first differences, although correctly specified for covariance-stationary series, would **not** capture this long-term relationship. In such cases, a lagged error-correction term would need to be added to the model after fitting it to the first differences of non-stationary variables [2].

3.2.2 Granger Causality Analysis

There is often a lack of consensus in the empirical literature regarding the relationship and direction of causality between oil prices and the Real Trade Weighted U.S. Dollar Index, particularly across different countries. Several factors contribute to this uncertainty: (i) Ferraro, Rogoff, and Rossi [10] argued that while commodity prices, including oil, contain significant information for predicting exchange rates at the daily frequency, their predictive power at the monthly or quarterly frequency is much lower, especially for smaller oil-exporting countries. Thus, data frequency plays a critical role when analysing the direction of causality; (ii) a country's oil dependence over time. For instance, Ferraro, Rogoff, and Rossi [10] demonstrated that the predictive power of oil prices for Canada's exchange rates improved once Canada became a net oil-exporting

country; and (iii) the time period of data under analysis. For example, Coudert and Mignon [6] found a negative relationship between real oil prices and the U.S. real effective exchange rate from 1974 to 2015. However, this relationship becomes positive when the series under consideration ends in the mid-2000s [5].

To determine which variables predict the movements of the others, the analysis focused on establishing the correct variables for the recursive model, as outlined by Castro and Jiménez-Rodríguez [5]. A linear Granger-causality test was first applied between the log of WTI Crude Oil prices and the log of the Real Trade Weighted U.S. Dollar Index, using the `grangercausalitytests` method from Statsmodels [21]. Granger-causality tests assess whether past values of one variable can help predict future values of another, but they do not provide insights into the true causal relationship between variables [8].

The linear Granger-causality test involves fitting autoregressive models to two time series, Y_t (the potential effect) and X_t (the potential cause). These models are represented as

$$Y_t = c_1 + \sum_{i=1}^{p} \alpha_{1,i} Y_{t-i} + \sum_{i=1}^{p} \beta_{1,i} X_{t-i} + \epsilon_{y,t}, \tag{3.2}$$

$$X_t = c_2 + \sum_{i=1}^{p} \alpha_{2,i} X_{t-i} + \sum_{i=1}^{p} \beta_{2,i} Y_{t-i} + \epsilon_{x,t}, \tag{3.3}$$

where p represents the autoregressive order, α_1, α_2, β_1, and β_2 are the coefficients to be estimated, and ϵ_t and η_t are error terms. The null hypothesis of the test is that X_t does not Granger-cause Y_t, tested using the F-statistic, which measures how much better the unrestricted model (with both X_t and Y_t) fits the data compared to the restricted model (without X_t).

The F-statistic is given by

$$F = \frac{\mathrm{RSS}_r - \mathrm{RSS}_u}{\mathrm{RSS}_u/(n-k)}, \tag{3.4}$$

where RSS_r and RSS_u are the residual sum of squares for the restricted and unrestricted models, respectively, n is the number of observations, and k is the number of regressors in the unrestricted model. If the computed F-statistic yields a p-value less than the chosen significance level (e.g., 0.05), the null hypothesis is rejected, providing evidence of Granger-causality.

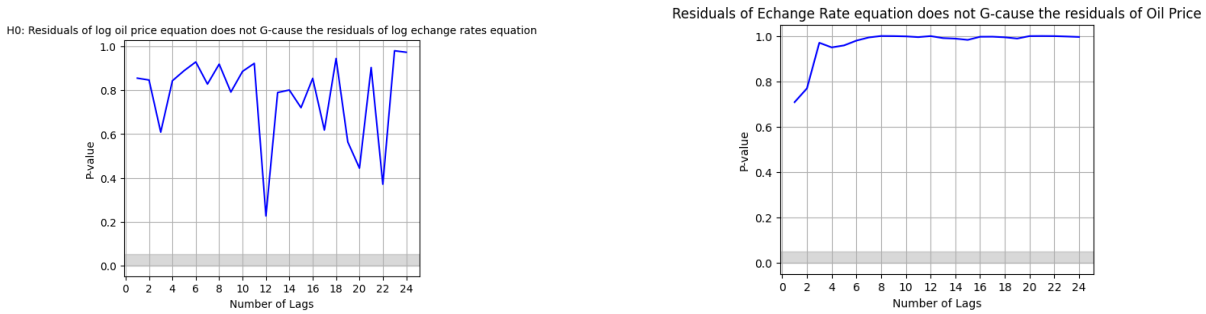

Figure 3: Plot (left) shows the p-values for testing nonlinear Granger-causality between the residuals of the Log Oil Price and Log Exchange Rate equations. The shaded area highlights significant p-values (≤ 0.05), indicating potential nonlinear causal relationships. The analysis spans up to 24 lags, with the p-values plotted against the number of lags. Plot (right) illustrates the inverse relationship.

In Figure **??**, plot (a) shows that the null hypothesis that oil prices do not Granger-cause exchange rates is rejected at the 5% level when the lag order, p, is between 6 and 13. In contrast, reverse causality is not observed. However, linear Granger-causality tests may not fully capture non-linear dynamics. As such, a nonlinear Granger-causality test, proposed by Diks and Panchenko [7], was conducted. The time series were first differentiated, and a VAR model with $p = 2$ was applied, based on the Bayesian Information Criterion (BIC), which is defined as

$$\text{BIC} = k \ln n - 2 \ln \hat{L}, \tag{3.5}$$

where $\hat{L}$ is the maximised value of the likelihood function, n is the number of data points, and k is the number of parameters [22].

The BIC addresses the issue of overfitting by introducing a penalty term for the number of parameters in the model. The residuals from the oil price and exchange rate equations were then calculated, and a nonlinear Granger-causality test was applied to assess the incremental predictive power of the residuals beyond the linear relationships captured by the VAR model. As Hiemstra and Jones [15] explained, by "removing linear predictive power with a linear VAR model, any remaining predictive power can be considered nonlinear." This was implemented using the `nonlincausality` Python package [20].

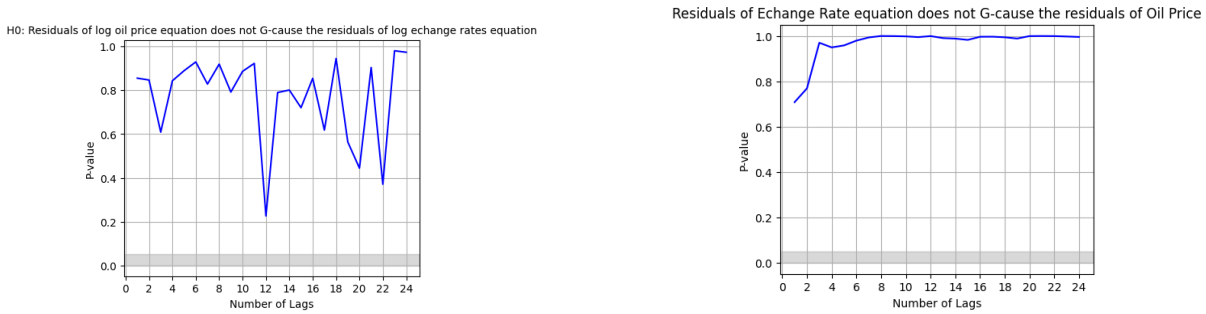

Figure 4: Panel (left) shows the p-values for testing nonlinear Granger-causality between the residuals of the Log Oil Price and Log Exchange Rate equations. The shaded area highlights significant p-values (≤ 0.05), indicating potential nonlinear causal relationships. The analysis spans up to 24 lags, with the p-values plotted against the number of lags. Panel (right) illustrates the inverse relationship.

Figure 4 presents the p-values for up to 24 lags. In both directions, the null hypothesis that the residuals of the oil price equation do not Granger-cause the residuals of the exchange rate equation cannot be rejected, and the reverse is also true.

In conclusion, the only Granger-causality found was linear Granger-causality from the log of oil prices to the log of exchange rates. This suggests that the order of variables in the VAR models should place oil prices O_t before exchange rates ER_t when modelling the relationship, as oil prices appear to respond to exchange rates with a delay.

3.2.3 Time-invariant VAR Model

The concepts used to define a bi-variate VAR model, estimate reduced-form parameters, and determine impulse response functions (IRFs) are drawn from the work of Kotzé [17]. In this section, a bi-variate model is defined for $y_{1,t}$ and $y_{2,t}$ to account for *contemporaneous* variables—those measured simultaneously. The variable $y_{1,t}$ can be influenced by both past and current realisations of $y_{2,t}$, and vice versa. The structural form of the model is given as

$$\begin{aligned} y_{1,t} &= b_{10} - b_{12}y_{2,t} + \gamma_{11}y_{1,t-1} + \gamma_{12}y_{2,t-1} + \varepsilon_{1,t}, \\ y_{2,t} &= b_{20} - b_{21}y_{1,t} + \gamma_{21}y_{1,t-1} + \gamma_{22}y_{2,t-1} + \varepsilon_{2,t}, \end{aligned} \tag{3.6}$$

where $y_{1,t}$ and $y_{2,t}$ are assumed to be stationary, and the components of ε_t, namely $\varepsilon_{1,t}$ and $\varepsilon_{2,t}$, are white noise with constant variance terms σ_1 and σ_2. It is further assumed that $\varepsilon_{1,t}$ and $\varepsilon_{2,t}$ are uncorrelated, enabling the identification of independent shocks, which are analysed and plotted for oil and exchange rates in this section. The

covariance matrix of the error terms is given as

$$\Sigma_\varepsilon \sim \begin{bmatrix} \sigma_1 & 0 \\ 0 & \sigma_2 \end{bmatrix}. \tag{3.7}$$

In this model, the coefficient b_{12} captures the contemporaneous effect of a change in $y_{2,t}$ on $y_{1,t}$, while b_{21} captures the reverse relationship.

The structural form can be expressed in its reduced form as

$$B\mathbf{y}_t = \Gamma_0 + \Gamma_1 \mathbf{y}_{t-1} + \varepsilon_t, \tag{3.8}$$

where

$$B = \begin{bmatrix} 1 & b_{12} \\ b_{21} & 1 \end{bmatrix}, \mathbf{y}_t = \begin{bmatrix} y_{1,t} \\ y_{2,t} \end{bmatrix}, \Gamma_0 = \begin{bmatrix} b_{10} \\ b_{20} \end{bmatrix}, \Gamma_1 = \begin{bmatrix} \gamma_{11} & \gamma_{12} \\ \gamma_{21} & \gamma_{22} \end{bmatrix}, \varepsilon_t = \begin{bmatrix} \varepsilon_{1,t} \\ \varepsilon_{2,t} \end{bmatrix}.$$

Premultiplying by B^{-1} yields the reduced-form VAR model

$$\mathbf{y}_t = A_0 + A_1 \mathbf{y}_{t-1} + u_t, \tag{3.9}$$

where $A_0 = B^{-1}\Gamma_0$, $A_1 = B^{-1}\Gamma_1$, and $u_t = B^{-1}\varepsilon_t$.

In the reduced-form VAR model, Cholesky decomposition is crucial for identifying the causal relationships between variables and determining the IRFs. Cholesky decomposition decomposes the variance-covariance matrix of the error terms into a lower triangular matrix, enabling the identification of contemporaneous effects between the variables.

The ordering of variables in the VAR model is important when using Cholesky decomposition. Endogenous variables are influenced by other variables within the system, while exogenous variables are not. Based on the Granger-causality analysis, the exchange rate is considered endogenous, as past values of oil prices and exchange rates improve the prediction of future exchange rates. Oil prices are treated as exogenous, as they are not directly influenced by exchange rates in the short term. This finding, although debatable, is used in our VAR model and will be discussed further in the Discussion section.

The lower triangular matrix resulting from Cholesky decomposition determines the contemporaneous relationships between variables, ordering them based on exogeneity. The most exogenous variable is placed first, and the most endogenous variable is placed last. Cholesky decomposition imposes restrictions on contemporaneous relationships through recursive identification.

In impulse response analysis, the order of variables dictates the direction of causality. For instance, if y_1 is placed before y_2 in the VAR model, applying Cholesky decomposition implies that y_1 is more exogenous and has a contemporaneous effect on y_2,

but not vice versa. This ensures that IRFs accurately reflect the causal relationships identified by the model.

Mathematically, Cholesky decomposition can be expressed as

$$\Sigma = \mathbf{L}\mathbf{L}^{\mathbf{T}}, \tag{3.10}$$

where Σ is the variance-covariance matrix of the error terms, and $\mathbf{L}$ is the lower triangular matrix from the decomposition.

To select the appropriate order for the VAR model, we fitted increasing orders of the VAR model and chose the order that minimised the Akaike Information Criterion (AIC), which is defined as

$$\text{AIC} = -2\ln(L) + 2k, \tag{3.11}$$

where L is the likelihood of the model and k is the number of parameters.

The AIC values for various lag orders are shown in Table 2. The optimal lag order is $p = 2$, as it minimizes the AIC.

Lag Order, p	**AIC**	**BIC**	**FPE**	**HQIC**
0	-13.92	-13.90	9.000e-07	-13.91
1	-14.12	-14.06	7.342e-07	-14.10
2	**-14.13***	-14.03	7.299e-07	-14.09
3	-14.13	-13.98	7.320e-07	-14.07
4	-14.12	-13.94	7.371e-07	-14.05

Table 2: Selection criteria values for different lag order values (p) in the VAR model. The values in bold with * indicate the minimum values for each criterion.

The lag order $p = 2$ was selected for the VAR model, aligning with results found in the literature, such as those reported by Fratzscher, Schneider, and Robays [11].

To illustrate how shocks in each variable propagate through the system, the VAR model is expressed in its moving average (MA) form. Just as every autoregressive model, AR(p), has a moving average representation, MA(q), every stable VAR(p) model has a vector moving average, VMA(q), representation:

$$\begin{bmatrix} y_{1,t} \\ y_{2,t} \end{bmatrix} = \begin{bmatrix} \mu_1 \\ \mu_2 \end{bmatrix} + \sum_{i=0}^{\infty} \begin{bmatrix} a_{11} & a_{12} \\ a_{21} & a_{22} \end{bmatrix}^i \cdot \begin{bmatrix} u_{1,t-i} \\ u_{2,t-i} \end{bmatrix}, \tag{3.12}$$

where μ_1 and μ_2 are the mean values of $y_{1,t}$ and $y_{2,t}$, respectively. Using the relationship between the structural and reduced forms of the model, the moving average representation of the SVAR model is derived, which describes the effect of a shock in ε_t on the endogenous variables.

The cumulative effects of shocks are described by the matrix Θ_i, which quantifies

how shocks $\varepsilon_{1,t}$ and $\varepsilon_{2,t}$ affect $y_{1,t}$ and $y_{2,t}$ over time. This matrix is defined as

$$\Theta_i = \begin{bmatrix} \theta_{1,1} & \theta_{1,2} \\ \theta_{2,1} & \theta_{2,2} \end{bmatrix}^i \cdot \frac{1}{1 - b_{12}b_{21}} \begin{bmatrix} 1 & -b_{12} \\ -b_{21} & 1 \end{bmatrix}. \tag{3.13}$$

Here, $\mu = [\mu_1 \ \mu_2]^T$ represents the mean values of $y_{1,t}$ and $y_{2,t}$. The endogenous variables $y_t = [y_{1,t} \ y_{2,t}]^T$ can thus be expressed as an infinite-order VMA process:

$$y_t = \mu + \sum_{i=0}^{\infty} \Theta_i \varepsilon_{t-i}. \tag{3.14}$$

This expression is useful for describing how shocks $\varepsilon_{1,t}$ and $\varepsilon_{2,t}$ impact the evolution of $y_{1,t}$ and $y_{2,t}$ over time. For example, $\theta_{12}(0)$ denotes the immediate effect of a one-unit change in $\varepsilon_{2,t}$ on $y_{1,t}$, while $\theta_{11}(1)$ represents the effect of a one-unit change in $\varepsilon_{1,t-1}$ on $y_{1,t}$ at the first lag.

3.3 Results

The IRFs in Figure 5 show the impact of a one standard deviation shock in each variable on the other or on itself. Panels (a) and (d) trace the impact of a shock to the oil price on itself and a shock to the exchange rate on itself, respectively. In both cases, the initial shock occurs in the first period and quickly dissipates as the impact returns to zero by the second period.

Figure 5(b) shows that a positive shock to the exchange rate significantly reduces the oil price. There is no first-period impact on the oil price, which reflects the restrictions imposed by the model. After approximately four periods (or months) of negative impact, the oil price returns to its initial level. Figure 5(c) demonstrates that a sudden increase in oil prices leads to an immediate depreciation of the exchange rate, with the effect dissipating after three periods.

The short-run reactions in Figures 5(b) and 5(c) are statistically significant, but the long-run responses are not. These findings support evidence of a negative relationship between oil prices and the real trade-weighted exchange rate, consistent with much of the existing literature.

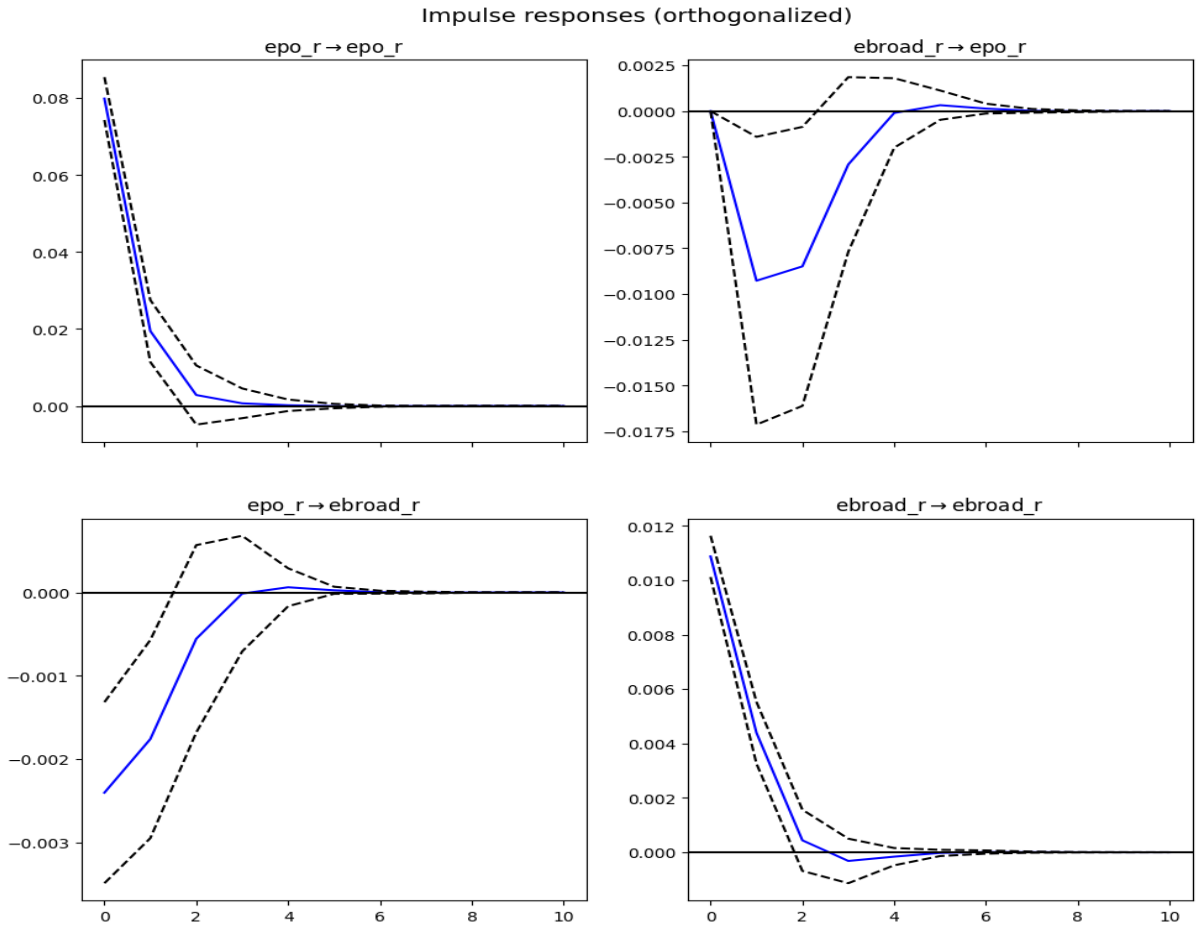

Figure 5: Plots showing the responses of each variable to a unit shock of the other variable in the time-invariant VAR model. The standard error bands use asymptotic standard errors to compute the confidence intervals, with a significance level of 95%. Panel (a) displays the impulse response of log oil price to itself. Panel (b) shows the impulse response of the log exchange rate to the log oil price. Panel (c) illustrates the impulse response of log oil price to log exchange rate, while panel (d) depicts the impulse response of log exchange rate to itself.

4 Conclusion

This study highlights the significant role of the U.S. as a major trading hub and key player in global energy markets. Given that oil is predominantly traded in USD, we explored the impact of USD exchange rate fluctuations on oil prices using a time-invariant VAR model. The analysis, covering data from 1986 to 2019, revealed that a sudden appreciation in the USD leads to a significant decline in oil prices, aligning with existing research. As the USD appreciates, foreign economies face higher costs for purchasing oil, reducing demand and thereby lowering prices. Furthermore, an oil price shock was found to induce a temporary negative reaction in the USD exchange rate, converging to zero after approximately three months.

However, the time-invariant nature of the VAR model presents limitations, particularly in its assumption that shocks remain constant over time. To address this, future research could adopt a time-variant VAR model, allowing for dynamic standard deviations that better reflect changes in market conditions. Such an approach would enhance the realism of shock responses, accounting for varying market environments. Additional improvements could involve analysing how exchange rates and oil prices react to shocks during periods of extreme market movements, and identifying the underlying causes of oil price shocks. Understanding these relationships would offer more nuanced insights into the impact of oil price fluctuations on broader economic and industrial activity.

References

[1] Bank for International Settlements. *Broad Effective Exchange Rate for United States [NBUSBIS]*. URL: https://fred.stlouisfed.org/series/NBUSBIS.

[2] Christopher F. Baum. *VAR, SVAR and VECM models*. EC 823: Applied Econometrics. 2013. URL: http://fmwww.bc.edu/EC-C/S2013/823/EC823.S2013.nn10.slides.pdf.

[3] Carol C. Bertaut, Bastian von Beschwitz, and Stephanie E. Curcuru. "The International Role of the U.S. Dollar". In: *FEDS Notes* (Oct. 2021). URL: https://doi.org/10.17016/2380-7172.2998.

[4] Martin Bodenstein, Christopher J Erceg, and Luca Guerrieri. "Oil shocks and external adjustment". In: *Journal of International Economics* 83.2 (2011), pp. 168–184. DOI: 10.1016/j.jinteco.2010.10.006.

[5] Cesar Castro and Rebeca Jiménez-Rodríguez. "Dynamic interactions between oil price and exchange rate". In: *PLoS One* 15.8 (Aug. 2020), e0237172. DOI: 10.1371/journal.pone.0237172.

[6] Virginie Coudert and Valérie Mignon. "Reassessing the empirical relationship between the oil price and the dollar". In: *Energy Policy* 95 (2016), pp. 147–157. DOI: 10.1016/j.enpol.2016.05.002.

[7] Cees Diks and Valentyn Panchenko. "A new statistic and practical guidelines for nonparametric Granger causality testing". In: *Journal of Economic Dynamics and Control* 30 (2006), pp. 1647–1669. DOI: 10.1016/j.jedc.2005.08.008.

[8] Eric. *Introduction to Granger Causality*. https://www.aptech.com/blog/introduction-to-granger-causality/. Published June 29, 2021. Updated October 4, 2021. 2021.

[9] Eric. *Unit Root Tests with Structural Breaks*. 2019. URL: https://www.aptech.com/blog/unit-root-tests-with-structural-breaks/.

[10] D. Ferraro, K. Rogoff, and B. Rossi. "Can oil prices forecast exchange rates? An empirical analysis of the relationship between commodity prices and exchange rates". In: *Journal of International Money and Finance* 54 (2015), pp. 116–141. DOI: 10.1016/j.jimonfin.2015.03.001.

[11] Marcel Fratzscher, Daniel Schneider, and Ine Van Robays. *Oil prices, exchange rates and asset prices*. Tech. rep. 1689. ECB Working Paper Series, 2014.

[12] Marko Gränitz. *Long-term investment trends: the crude oil boom in the 2000s*. https://www.lgt.com/global-en/market-assessments/insights/financial-markets/long-term-investment-trends-the-crude-oil-boom-in-the-2000s-20108. Sept. 2020.

[13] Francesco Guerrera. "Why the dollar keeps winning in the global economy". In: *Breakingviews* (Feb. 2023). URL: https://www.reuters.com/breakingviews/global-markets-breakingviews-2023-02-28/.

[14] Adam Hayes. *What Is the Real Effective Exchange Rate (REER) and Its Equation?* Updated June 30, 2021. URL: https://www.investopedia.com/terms/r/reer.asp.

[15] Craig Hiemstra and J. David Jones. "Testing for Linear and Nonlinear Granger Causality in the Stock Price-Volume Relation". In: *The Journal of Finance* 49.5 (1994), pp. 1639–1664. DOI: 10.2307/2329266.

[16] jkclem. *jkclem/chowtest*. https://github.com/jkclem/chowtest/tree/master. Accessed: 2024 April. 2022.

[17] Kevin Kotzé. *Structural Vector Autoregression Models*. https://kevin-kotze.gitlab.io/tsm/ts-11-note/. Accessed on 27 April 2024.

[18] Daiki Maki. "Tests for cointegration allowing for an unknown number of breaks". In: *Economic Modelling* 29.5 (2012), pp. 2011–2015.

[19] F. Pedregosa et al. "Scikit-learn: Machine Learning in Python". In: *Journal of Machine Learning Research* 12 (2011), pp. 2825–2830.

[20] Maciej Rosoł, Marcel Młyńczak, and Gerard Cybulski. "Granger causality test with nonlinear neural-network-based methods: Python package and simulation study". In: *Computer Methods and Programs in Biomedicine* 216 (2022). DOI: 10.1016/j.cmpb.2022.106669.

[21] Skipper Seabold and Josef Perktold. "statsmodels: Econometric and statistical modeling with python". In: *Proceedings of the 9th Python in Science Conference*. 2010.

[22] Petre Stoica and Yalcin Selen. "Model-order selection: a review of information criterion rules". In: *IEEE Signal Processing Magazine* (July 2004), pp. 36–47. DOI: 10.1109/MSP.2004.1311138.

[23] C. Truong, L. Oudre, and N. Vayatis. "Selective review of offline change point detection methods". In: *Signal Processing* 167 (2020), p. 107299.